








RAPID COMMUNICATION | JANUARY 04 2024

Direct measurement of built-in electric field inside a 2D cavity

Special Collection: [2023 JCP Emerging Investigators Special Collection](#)

Li Li ; Jinyang Ling ; Dongxu Zhang ; Nanyang Wang; Jiamin Lin ; Zhonghua Xi ; Weigao Xu  

 Check for updates

J. Chem. Phys. 160, 011102 (2024)

<https://doi.org/10.1063/5.0180444>

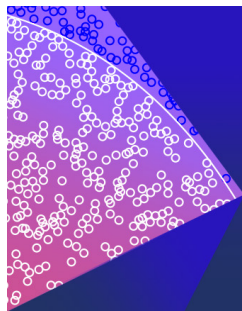


View
Online



Export
Citation

CrossMark



The Journal of Chemical Physics

Special Topic: Monte Carlo methods,
70 years after Metropolis *et al.* (1953)

Submit Today

 AIP
Publishing

 AIP
Publishing

Direct measurement of built-in electric field inside a 2D cavity

Cite as: J. Chem. Phys. 160, 011102 (2024); doi: 10.1063/5.0180444

Submitted: 9 October 2023 • Accepted: 27 November 2023 •

Published Online: 4 January 2024



View Online



Export Citation



CrossMark

Li Li,¹  Jinyang Ling,¹  Dongxu Zhang,¹  Nanyang Wang,² Jiamin Lin,¹  Zhonghua Xi,¹ 
and Weigao Xu^{1,a)} 

AFFILIATIONS

¹Key Laboratory of Mesoscopic Chemistry, School of Chemistry and Chemical Engineering, Nanjing University, Nanjing 210023, China

²National Laboratory of Solid State Microstructures, College of Engineering and Applied Sciences, Nanjing University, Nanjing 210023, China

Note: This paper is part of the 2023 JCP Emerging Investigators Special Collection.

^{a)}**Author to whom correspondence should be addressed:** xuwg@nju.edu.cn

ABSTRACT

The on-demand assembly of 2D heterostructures has brought about both novel interfacial physical chemistry and optoelectronic applications; however, existing studies rarely focus on the complementary part—the 2D cavity, which is a new-born area with unprecedented opportunities. In this study, we have investigated the electric field inside a spacer-free 2D cavity consisting of a monolayer semiconductor and a gold film substrate. We have directly captured the built-in electric field crossing a blinking 2D cavity using a Kelvin probe force microscopy–Raman system. The simultaneously recorded morphology (M), electric field (E), and optical spectroscopy (O) mapping profile unambiguously reveals dynamical fluctuations of the interfacial electric field under a constant cavity height. Moreover, we have also prepared non-blinking 2D cavities and analyzed the gap-dependent electric field evolution with a gradual heating procedure, which further enhances the maximum electric field exceeding 10^9 V/m. Our work has revealed substantial insights into the built-in electric field within a 2D cavity, which will benefit adventures in electric-field-dependent interfacial sciences and future applications of 2D chemical nanoreactors.

Published under an exclusive license by AIP Publishing. <https://doi.org/10.1063/5.0180444>

INTRODUCTION

Aside from the remarkable progress on two-dimensional (2D) materials *per se*,^{1–5} as the complementary part, 2D empty spaces or 2D cavities⁶ have come into sight with both interesting science^{7–11} and appealing application capacities.^{12–15} Pioneering studies include the investigation of difficult problems that are otherwise inaccessible, e.g., capillary condensation of discrete water molecules under atomic scale confinement,⁷ ultralow dielectric response of interfacial water,⁸ and frictionless or even ballistic transport of water⁹ and helium gas¹⁰ in graphene or hexagonal boron nitride (h-BN) cavities. Moreover, 2D cavities are considered as promising ion-filters for seawater desalination¹² and confined nanoreactors^{13–15} for CO oxidation.

Van der Waals assembled 2D cavities provide an ideal platform for exploring the physical properties and functionalities of matters under planar constraints; however, the measurement of inherent multiple physical fields and the associated interface effects

in such 2D empty spaces is extremely lacking. With the placement of pressure-sensitive molecules, the hydrostatic pressure inside a graphene–graphene cavity is estimated to be around 10 000 atm.¹⁶ However, other static fields, such as electric-, magnetic-, and thermal-fields, under such atomically confined conditions are little touched. This is mainly because of the natural complexity and susceptibility of nanoscale cavities. More challengingly, since the limited overlapping of electronic wavefunctions between the two components,^{17,18} there would be quantum fluctuations on charge transfer channels,^{19–22} which cause spatiotemporal inhomogeneities in certain physical fields.

In this work, we tackled the above-mentioned issue through *in situ* spatiotemporal investigations on a series of spacer-free 2D cavities with a coupled Kelvin probe force microscopy (KPFM)–Raman system. By introducing an M (morphology)–E (electric field)–O (optical spectroscopy) mapping method (Fig. 1), we monitored the morphology, in particular the height variations, and conducted the surface potential measurement, which repre-

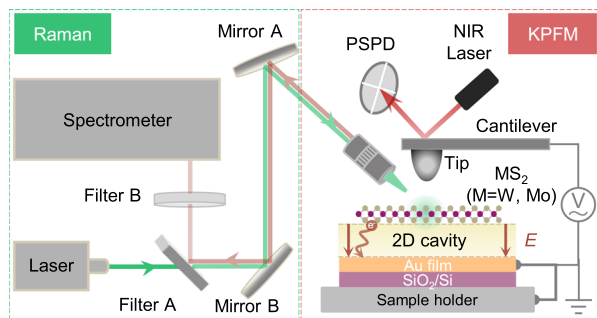


FIG. 1. Schematic illustration of the M–E–O mapping system. A Raman spectrometer is coupled with KPFM under a side-reflection mode. An empty space is formed between the monolayer semiconductor (WS_2 or MoS_2) and the Au substrate. The morphology (M), electric field (E), and optical spectroscopy (O) signals can be synchronously collected.

sents the amount of charge flow within the cavities. We performed the *in situ* optical spectroscopic mapping on the Raman spectroscope, which provides dynamic fluorescence information. Through M–E–O mapping, we have directly captured the dynamic fluctuations of the interfacial electric field for the first time. Meanwhile, we have made substantial efforts toward a quantitative understanding of

the gap-dependent electric field inside the 2D cavity. We expect that our work will stimulate attention and progress in the built-in electric field associated with catalysis^{23,25} and energy conversion,^{26,27} further promoting the design and application of 2D cavities.

RESULTS AND DISCUSSION

We have chosen to investigate WS_2/Au and MoS_2/Au 2D cavities in our experiments. This is because of at least three reasons: (i) spacer-free structure reserving space for the potential fillings, such as nanoparticles and molecules; (ii) the intrinsic significance of a semiconductor–metal interface, which is intimately associated with optoelectronic^{28,29} and catalytic applications;^{30–32} and (iii) such cavities have been found to exhibit spontaneously fluctuations with time,^{19–21} offering exotic opportunities to understand dynamic interface processes.

Preparation and single-channel characterization of 2D cavities

Mechanically exfoliated monolayer WS_2 flakes were carefully transferred onto a gold substrate using a polydimethylsiloxane (PDMS)-assisted procedure,³³ resulting in the formation of a 2D WS_2/Au interface. By measuring the atomic force microscope (AFM) height profile, we can see that a flawless 2D cavity is formed,

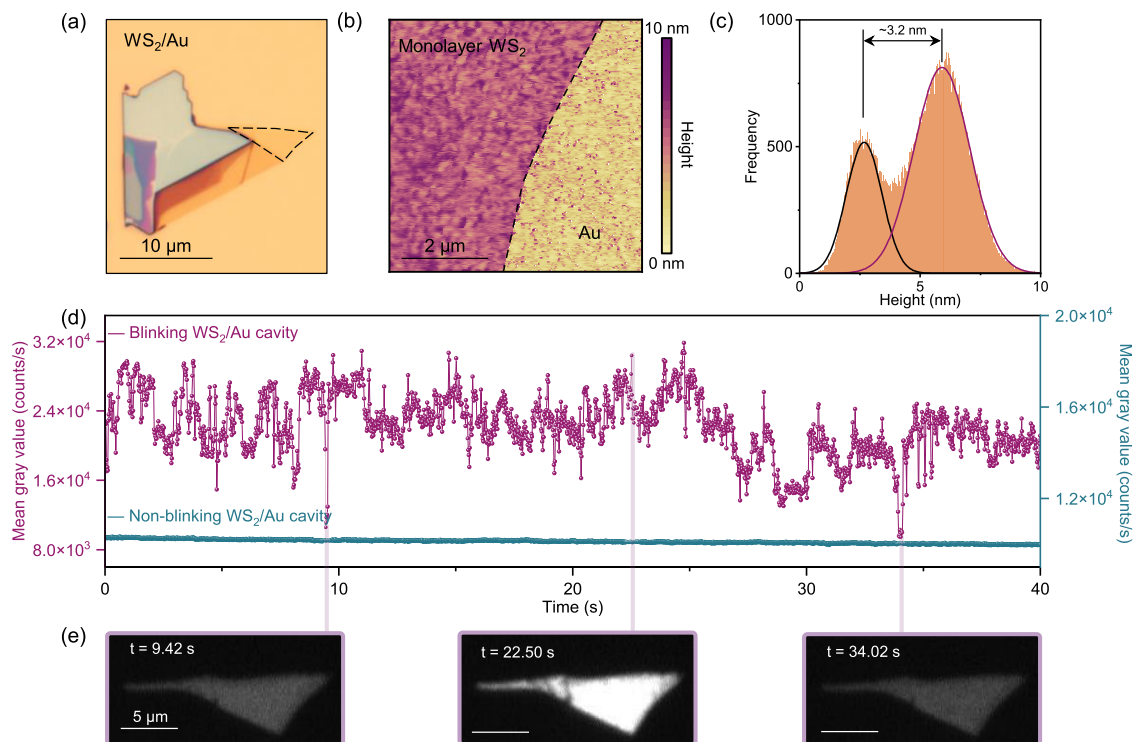


FIG. 2. Morphology and fluorescence properties of a blinking 2D cavity. (a) Optical image of a spacer-free WS_2/Au cavity. The dashed region indicates the monolayer of WS_2 . (b) Surface morphology of the monolayer WS_2 and Au substrate. (c) Histogram of frequency distribution corresponds to (b). (d) Grayscale intensity of a blinking and a non-blinking WS_2/Au cavity over time. Time interval, 20 ms. (e) Typical fluorescence images of a bright state ($t = 22.50$ s) and two dark states ($t = 9.42, 34.02$ s) of a blinking cavity.

with a clear boundary between the WS₂ region and the Au substrate region [Fig. 2(b)]. Here, we use $h_{\text{cavity}} = h_{\text{WS}_2} - \langle h_{\text{Au}} \rangle$ to describe the global structure of this 2D cavity, where the average cavity height h_{cavity} can be calculated by subtracting the mean height value of the Au substrate from the measured height value of the WS₂ layer. As shown in Fig. 2(c), the as-prepared WS₂/Au cavity exhibited an average height of ~ 3.2 nm. This value is much larger than the equilibrium interlayer spacing of 2D WS₂ crystals (~ 0.7 nm),³⁴ suggesting the spontaneous formation of a cavity-like structure. Based on our recent results, such spacer-free cavities can survive for years under ambient conditions, which is in line with our previous studies on weakly coupled 2D heterostructures.^{19,21} According to height measurements on fifteen WS₂/Au cavities, all of them show such cavity-like structures and their average height varies from 1.9 to 3.8 nm (Fig. S1).

We first focus on the optical properties of these 2D cavities. With the aid of a wide-field fluorescence microscope, we found that about 15% of the as-prepared WS₂/Au cavities exhibit prominent fluorescence blinking,²⁰ while the rest show stable fluorescence emission. Currently, we are not able to fully control the preparation procedure to selectively get blinking or non-blinking cavities; we found that samples with flat edges might be necessary for the observation of large fluorescence fluctuations. Here, we will start with the more challenging part, i.e., dynamical monitoring of the fluctuating electric field of blinking 2D cavities, and the constant electric field and gap-dependence in the non-blinking cavities will be discussed in the second part.

A typical time-dependent emission profile of a blinking WS₂/Au cavity is plotted in Fig. 2(d). As one of the mysterious features of blinking 2D cavities, the emission pattern varies globally with clear boundaries. Three typical snapshots at 9.42, 22.50, and 34.02 s are shown in Fig. 2(e), which corresponds to a bright state ($t = 22.50$ s) and two dark states ($t = 9.42$ and 34.02 s). To gain insights into the collective behavior at a microscopic level, we further acquired the fluorescence spectra over time and plotted them on a 2D colored map (Fig. S2a); the alternating bright (purple) and dark (yellow) streaks clearly show the blinking feature of the WS₂/Au cavity. Employing a batch-fitting treatment on each spectrum, we obtain dynamical evolutions of the emission of neutral excitons (A) and charged excitons (or called trions, A⁻). We found a distinct time-dependence of A⁻ and A excitons, where A⁻ peak shifts from 1.970 to 2.007 eV, while A remains unchanged at 2.017 eV, as shown in Fig. S2b. The dynamic fluctuations of A⁻ and A excitons can be understood from an intermittent interlayer charge transfer mechanism.^{19,21} Notably, charge transfer within a 2D cavity shall be directly related to the interfacial carrier accumulation and, thus, the resulting built-in electric field. Therefore, blinking electric fields, raised from the limited overlap of electronic wavefunctions between the monolayer semiconductor and the Au substrate, shall be an inherently important characteristic of 2D cavities. In the following text, we will introduce the M–E–O mapping method to trace the hidden details of interfacial fluctuation event and the resulting vertical electric field across the 2D cavities.

M–E–O mapping of a blinking 2D cavity

We employed a KPFM–Raman system to simultaneously collect the morphology, the surface potential, and the fluorescence

spectra. The global fluctuation feature of the 2D cavity allows us to investigate the surface potential and fluorescence variation of the entire sample from a single measurement point. Here, we have adopted a one-line-scan mode [Fig. 3(a)] in our *in situ* M–E–O measurement to track tiny morphology variations. We chose to record a line profile over time to form a pseudo-2D map. As shown in Fig. 3(b), the x axis corresponds to position coordinates, while the y axis represents the sequential scan number, ranging from the 1st to the 100th scan. We have intentionally selected a target line-profile with distinct ripples, where the height profile has several characteristic peaks (purple lines). We found that the morphology of the 2D cavity remains unchanged throughout the scanning process (~ 200 s), except for a slight bending of the peak trajectory caused by a thermal drift [Fig. 3(b)]. The height profile with reproducible characteristic features serves as a natural internal-marker to simultaneously monitor the surface potential and fluorescence blinking events.

Then, we turn to check the corresponding surface potential and optical spectroscopy features. Before we start, it shall be mentioned that Shafran *et al.*³⁵ and He *et al.*³⁶ have implemented pioneering studies in which an AFM tip was employed to modulate the emission properties of quantum dot and 2D semiconductors. In our work, we want to focus on the intrinsic electric field within the 2D cavity, and thus, the AFM tip was intentionally lifted by ~ 15 nm to minimize possible perturbation to the cavity. By examining the state distribution in blinking profiles when the AFM tip is either absent or operating (Fig. S3), no apparent tip-induced perturbations were observed.

As illustrated in Figs. 3(c) and 3(d), in stark difference with the surface morphology map, under continuous photoexcitation, the corresponding contact potential difference (CPD) map and the fluorescence intensity map do display distinct fluctuations; three typical jumps are labeled as (i), (ii), and (iii), respectively. To be noted, such jumps are not from non-linear tip–sample interactions, since in such cases, the jumps shall appear in both the morphology and CPD maps (Fig. S4). The correlated CPD and fluorescence fluctuations suggest that the unexpected jumps shall come from long-range and random charge transfer events within the blinking 2D cavity. Event (i) in Fig. 3(c) represents a bright event (purple line; the CPD value of WS₂ increases), indicating that there is an outflow of electrons from the monolayer WS₂ to the Au substrate. This causes a decreased electron concentration in WS₂ (an n -type semiconductor in our experiments) and will boost fluorescence emission (corresponds to a bright fluorescence state).²¹ Indeed, we do have observed a positive correlation of CPD values and fluorescence intensities [Figs. 3(c) and 3(d)].

Notably, there is a long-term puzzle regarding the origin of blinking phenomenon in 2D materials. One of the hypotheses is that there might be a global “breathing” effect within the 2D cavity, i.e., blinking events take place when there is a cavity height variation. Based on the above-mentioned M–E–O mapping results, an unambiguous answer to this hypothesis can be given: fluorescence fluctuation is an intrinsic property of 2D cavities and is not caused by the global cavity height variation. It sounds to be a good news, as we can take the cavity height as a constant value even when dealing with cavities showing spatiotemporal fluctuations; thus, the measurement of the electric field ($E = U/d$) can be simplified. We then evaluate the built-in electric field in the blinking WS₂/Au cavity shown in Fig. 3.

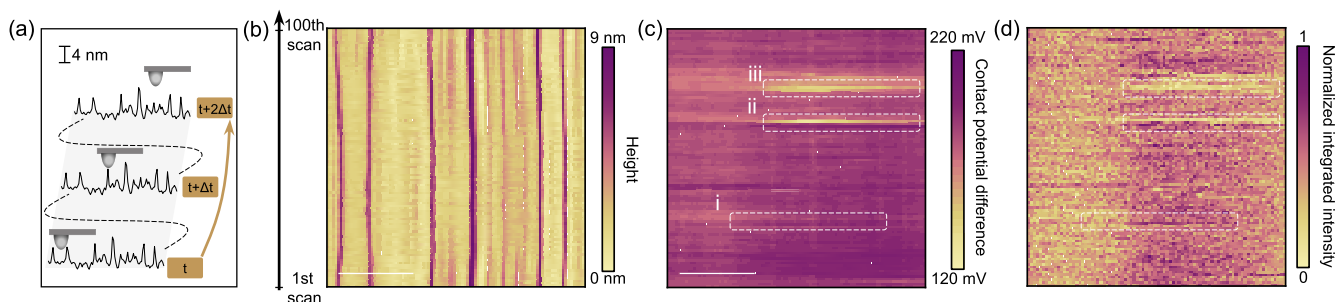


FIG. 3. M–E–O mapping of a blinking 2D cavity. (a) Schematic diagram of the one-line-scan mode, height bar 4 nm. (b)–(d) A M–E–O mapping for (b) morphology, (c) surface potential, and (d) normalized PL emission. In panels (b) and (c), the scale bar is 1 μm . The synchronous bright and dark streaks (labeled as i, ii, and iii) in panels (c) and (d) show a positive correlation.

According to an average height (**d**) of 3.24 nm and a CPD difference value (U) of 80–180 mV, we will get a vertical electric field strength of 2.5×10^7 – 5.6×10^7 V/m. Specifically, three abrupt jumps show fluctuations in the CPD value [Fig. 3(c)], +20 mV (i), –35 mV (ii), and –22 mV (iii), and their corresponding electric field changes are $+6.2 \times 10^6$ V/m, -1.1×10^7 V/m, and -6.8×10^6 V/m. A statistical analysis of the absolute value of ΔCPD on three blinking cavities is plotted in Fig. S5.

Quantitative investigation on gap-dependent electric field in 2D cavities

Despite the fact that the quantum fluctuations are vital parts of the intrinsic properties of 2D cavities, one may want to know whether we can prepare 2D cavities with stable and controllable electric fields. In this part, we will investigate the gap-dependent electric field on the remaining non-blinking 2D cavities (~85%). Due to the spacer-free planar structure of the 2D cavities, precise height adjustment seems to be quite challenging. Luckily, we are able to continuously tune the cavity height after a gradual heating procedure. As shown in Fig. 4(a) (purple squares), the average height of the 2D cavities decreases monotonously with heating temperature. For the investigated WS_2/Au cavity at room temperature, the as-prepared state has an average height of 2.6 nm and gradually compresses to 1.7 nm. As the lower limit of height reaches the equilibrium interlayer spacing (~0.7 nm),³⁴ we chose to set the heat treatment threshold at 433 K. We also observed the appearance of bubble regions with out-of-plane deformations—mainly due to hydrocarbons;³⁷ after treatment above 393 K, such areas are excluded in our analyses as they are not the focus of this study (Fig. S6).

We then proceed to focus on the evolution of the built-in electric field during the compression of the 2D cavities. The final built-in electric field is determined by two variables: U and d , of which both are influenced by the heating treatment. As shown by the solid circles in Fig. 4(a), the average electric field has a non-monotonous dependence on the heating temperature. This non-monotonous relationship might be caused by a joint effect of the interfacial charge redistribution³⁸ and the cavity height.^{39,40}

In order to explore the electric field landscape inside 2D cavities, we plotted the 2D strength maps of the electric field in the

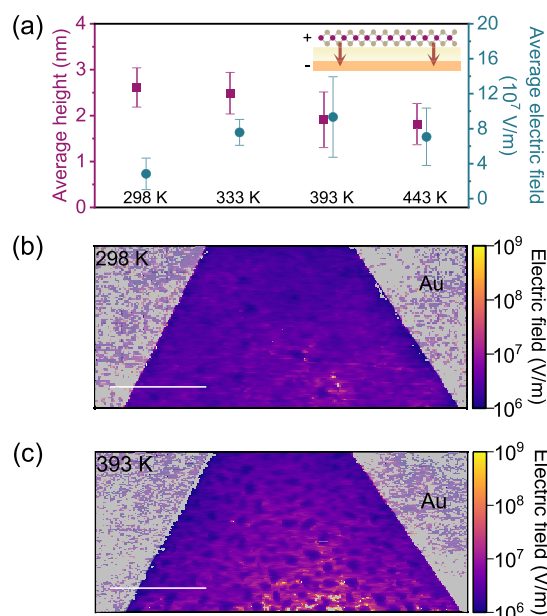


FIG. 4. Gap-dependent evolution of electric field in 2D cavities. (a) Scatter plots of the average electric field and the average height of 2D cavities annealed at 298, 333, 393, and 443 K in Ar gas for 20 min. (b) As-prepared at 298 K. (c) After annealing at 393 K. Spatial distribution map of the electric field in as-prepared 2D cavities (298 K) (b) and after annealing at 393 K (c). Scale bar, 1 μm .

WS_2/Au cavity annealed at 298 and 393 K, as shown in Fig. 4(b) and 4(c), respectively. The electric field distribution of the as-prepared 2D cavity spreads over the range of 10^6 – 10^7 V/m. After experiencing the heat treatment at 393 K, the 2D cavity exhibited an overall improvement of the electric field strength, even exceeding 10^9 V/m in some local areas. Interestingly, the electric field at the edges of the 2D cavity remains unchanged, and high electric fields tend to form at regions away from the boundaries. This may be related to boundary defect states with unstable dangling bonds. Moreover, the gradual heating treatment for optimizing the built-in electric field (exceeding 10^9 V/m) could be extended to other similar cavities, such as 2D MoS_2/Au cavities (Fig. S7). Such a high

strength of the electric field has already been demonstrated to be able to trigger and even control a series of chemical reactions, such as Diels–Alder reaction⁴¹ and oxidative C–H/N–H coupling.⁴²

CONCLUSIONS

We have successfully fabricated spacer-free 2D cavities and conducted *in situ* investigations into the dynamic behavior of the built-in electric field within these structures using a KPFM–Raman system. Through the application of M–E–O mapping, we have directly captured the dynamic fluctuating electric field for the first time, shedding light on the spatiotemporal inhomogeneity of nanoscale cavities. Furthermore, we have conducted a quantitative investigation of the gap-dependent electric field under gradual heating treatment and electric fields exceeding 10^9 V/m are realized and characterized. As a quick reference, supposing that the dipole difference between the ground state and the transition state of a molecule is about 5 D, a 2D cavity with an electric field of 1×10^9 V/m will result in a stabilization energy of about 2.4 kcal/mol, which can be adopted for the majority of polar chemical reactions.^{43,44} Moreover, introducing external laser fields might further enhance the electric field, thereby extending the range of chemical reactions that can be performed. Last but not least, benefited from the scalable CVD growth of 2D materials, we believe that our results and future efforts will help in the scalable preparation and applications of 2D nanoreactors.^{45–48}

SUPPLEMENTARY MATERIAL

The detailed sample fabrication, characterization, and data processing are available in the supplementary material.

ACKNOWLEDGMENTS

We acknowledge the financial support from the National Key R&D Program of China (Nos. 2020YFA0406104 and 2022YFA120470), the National Natural Science Foundation of China (Nos. 22333004, 22173044, and 21873048), and the Natural Science Foundation of Jiangsu Province (No. BK20220121).

AUTHOR DECLARATIONS

Conflict of Interest

The authors have no conflicts to disclose.

Author Contributions

L.L., N.W., and D.Z. fabricated the 2D cavities. L.L. and J.L. performed the KPFM–Raman measurements. L.L., J.L., and W.X. analyzed the data. J.L. and Z.X. contributed in the discussion. L.L. and W.X. wrote the manuscript. All authors have given approval to the final version of the manuscript.

Li Li: Conceptualization (equal); Data curation (lead); Investigation (lead); Methodology (lead); Visualization (lead); Writing – original draft (lead); Writing – review & editing (equal). **Jinyang Ling:** Data curation (supporting); Methodology (supporting); Writing – review & editing (supporting). **Dongxu Zhang:** Resources (supporting). **Nanyang Wang:** Resources (supporting). **Jiamin Lin:** Resources (supporting); Writing – review & editing (supporting). **Zhonghua Xi:** Resources (supporting). **Weigao Xu:** Conceptualization (equal); Data curation (supporting); Writing – review & editing (lead).

DATA AVAILABILITY

The data that support the findings of this study are available from the corresponding author upon reasonable request.

REFERENCES

- 1 K. S. Novoselov, A. K. Geim, S. V. Morozov, D. Jiang, Y. Zhang, S. V. Dubonos, I. V. Grigorieva, and A. A. Firsov, “Electric field effect in atomically thin carbon films,” *Science* **306**, 666–669 (2004).
- 2 K. S. Novoselov, D. Jiang, F. Schedin, T. J. Booth, V. V. Khotkevich, S. V. Morozov, and A. K. Geim, “Two-dimensional atomic crystals,” *Proc. Natl. Acad. Sci. U. S. A.* **102**, 10451–10453 (2005).
- 3 A. K. Geim and I. V. Grigorieva, “Van der Waals heterostructures,” *Nature* **499**, 419–425 (2013).
- 4 Y. Cao, V. Fatemi, S. Fang, K. Watanabe, T. Taniguchi, E. Kaxiras, and P. Jarillo-Herrero, “Unconventional superconductivity in magic-angle graphene superlattices,” *Nature* **556**, 43–50 (2018).
- 5 S. S. Fang, S. Duan, X. Z. Wang, S. J. Chen, L. Li, H. Li, B. C. Jiang, C. H. Liu, N. Y. Wang, L. Zhang, X. L. Wen, Y. G. Yao, J. Zhang, D. Q. Xie, Y. Luo, and W. G. Xu, “Direct characterization of shear phonons in layered materials by mechano-Raman spectroscopy,” *Nat. Photonics* **17**, 531–537 (2023).
- 6 A. K. Geim, “Exploring two-dimensional empty space,” *Nano Lett.* **21**, 6356–6358 (2021).
- 7 Q. Yang, P. Z. Sun, L. Fumagalli, Y. V. Stebunov, S. J. Haigh, Z. W. Zhou, I. V. Grigorieva, F. C. Wang, and A. K. Geim, “Capillary condensation under atomic-scale confinement,” *Nature* **588**, 250–253 (2020).
- 8 L. Fumagalli, A. Esfandiari, R. Fabregas, S. Hu, P. Ares, A. Janardanan, Q. Yang, B. Radha, T. Taniguchi, K. Watanabe, G. Gomila, K. S. Novoselov, and A. K. Geim, “Anomalously low dielectric constant of confined water,” *Science* **360**, 1339–1342 (2018).
- 9 B. Radha, A. Esfandiari, F. C. Wang, A. P. Rooney, K. Gopinadhan, A. Keerthi, A. Mishchenko, A. Janardanan, P. Blake, L. Fumagalli, M. Lozada-Hidalgo, S. Garaj, S. J. Haigh, I. V. Grigorieva, H. A. Wu, and A. K. Geim, “Molecular transport through capillaries made with atomic-scale precision,” *Nature* **538**, 222–225 (2016).
- 10 A. Keerthi, A. K. Geim, A. Janardanan, A. P. Rooney, A. Esfandiari, S. Hu, S. A. Dar, I. V. Grigorieva, S. J. Haigh, F. C. Wang, and B. Radha, “Ballistic molecular transport through two-dimensional channels,” *Nature* **558**, 420–424 (2018).
- 11 H. Li, J. Y. Ling, J. M. Lin, X. Lu, and W. G. Xu, “Interface engineering in two-dimensional heterostructures towards novel emitters,” *J. Semicond.* **44**, 011001 (2023).
- 12 A. Esfandiari, B. Radha, F. C. Wang, Q. Yang, S. Hu, S. Garaj, R. R. Nair, A. K. Geim, and K. Gopinadhan, “Size effect in ion transport through angstrom-scale slits,” *Science* **358**, 511–513 (2017).
- 13 R. Mu, Q. Fu, L. Jin, L. Yu, G. Fang, D. Tan, and X. Bao, “Visualizing chemical reactions confined under graphene,” *Angew. Chem., Int. Ed.* **51**, 4856–4859 (2012).
- 14 Y. H. Zhang, X. F. Weng, H. Li, H. B. Li, M. M. Wei, J. P. Xiao, Z. Liu, M. S. Chen, Q. Fu, and X. H. Bao, “Hexagonal boron nitride cover on Pt(111): A new route to tune molecule–metal interaction and metal-catalyzed reactions,” *Nano Lett.* **15**, 3616–3623 (2015).

- ¹⁵Y. Yao, Q. Fu, Y. Y. Zhang, X. Weng, H. Li, M. Chen, L. Jin, A. Dong, R. Mu, P. Jiang, L. Liu, H. Bluhm, Z. Liu, S. B. Zhang, and X. Bao, "Graphene cover-promoted metal-catalyzed reactions," *Proc. Natl. Acad. Sci. U. S. A.* **111**, 17023–17028 (2014).
- ¹⁶K. S. Vasu, E. Prestat, J. Abraham, J. Dix, R. J. Kashtiban, J. Beheshtian, J. Sloan, P. Carbone, M. Neek-Amal, S. J. Haigh, A. K. Geim, and R. R. Nair, "Van der Waals pressure and its effect on trapped interlayer molecules," *Nat. Commun.* **7**, 12168 (2016).
- ¹⁷C. H. Jin, E. Y. Ma, O. Karni, E. C. Regan, F. Wang, and T. F. Heinz, "Ultrafast dynamics in van der Waals heterostructures," *Nat. Nanotechnol.* **13**, 994–1003 (2018).
- ¹⁸R. Long and O. V. Prezhdo, "Quantum coherence facilitates efficient charge separation at a MoS₂/MoSe₂ van der Waals junction," *Nano Lett.* **16**, 1996–2003 (2016).
- ¹⁹W. Xu, W. Liu, J. F. Schmidt, W. Zhao, X. Lu, T. Raab, C. Diederichs, W. Gao, D. V. Seletskiy, and Q. Xiong, "Correlated fluorescence blinking in two-dimensional semiconductor heterostructures," *Nature* **541**, 62–67 (2017).
- ²⁰R. H. Godiksen, S. Wang, T. V. Raziman, M. H. D. Guimaraes, J. G. Rivas, and A. G. Curto, "Correlated exciton fluctuations in a two-dimensional semiconductor on a metal," *Nano Lett.* **20**, 4829–4836 (2020).
- ²¹H. Li, H. L. Li, X. Z. Wang, Y. F. Nie, C. Liu, Y. Dai, J. Y. Ling, M. N. Ding, X. Ling, D. Q. Xie, N. Lu, C. J. Wan, Q. H. Xiong, and W. G. Xu, "Spontaneous polarity flipping in a 2D heterobilayer induced by fluctuating interfacial carrier flows," *Nano Lett.* **21**, 6773–6780 (2021).
- ²²M. He, C. H. Ge, K. Braun, L. Y. Huang, X. Yang, H. P. Zhao, A. J. Meixner, X. Wang, and A. L. Pan, "Room temperature fluorescence blinking in MoS₂ atomic layers by single photon energy transfer," *Laser Photonics Rev.* **16**, 2200144 (2022).
- ²³X. Y. Luo, M. He, S. J. Hou, H. Zhou, K. Braun, X. L. Zhu, A. L. Pan, and X. Wang, "Realizing fluorescence blinking in monolayer MoSe₂ with the formation of 1D/2D heterostructure," *Adv. Funct. Mater.* (published online 2023).
- ²⁴F. He, Y. Lu, G. Jiang, Y. Zhang, P. Dong, X. Liu, Y. Wang, C. Zhao, S. Wang, X. Duan, J. Zhang, and S. Wang, "Unveiling the dual charge modulation of built-in electric field in metal-free photocatalysts for efficient photo-Fenton-like reaction," *Appl. Catal., B* **341**, 123307 (2024).
- ²⁵J. Zhang, X. Zhao, L. Chen, S. Li, H. Chen, Y. Zhu, S. Wang, Y. Liu, H. Zhang, X. Duan, M. Wu, S. Wang, and H. Sun, "Intrinsic mechanisms of morphological engineering and carbon doping for improved photocatalysis of 2D/2D carbon nitride van der Waals heterojunction," *Energy Environ. Mater.* **6**, e12365 (2022).
- ²⁶H. Chao, X. Luo, X. Yan, S. Wang, and J. Zhang, "Carbon nanofibers confined polyoxometalate derivatives as flexible self-supporting electrodes for robust sodium storage," *J. Colloid Interface Sci.* **654**, 107–113 (2024).
- ²⁷J. Zhang, K. Xie, Y. Jiang, M. Li, X. Tan, Y. Yang, X. Zhao, L. Wang, Y. Wang, X. Wang, Y. Zhu, H. Chen, M. Wu, H. Sun, and S. Wang, "Photoinducing different mechanisms on a Co-Ni bimetallic alloy in catalytic dry reforming of methane," *ACS Catal.* **13**, 10855–10865 (2023).
- ²⁸Q. H. Wang, K. Kalantar-Zadeh, A. Kis, J. N. Coleman, and M. S. Strano, "Electronics and optoelectronics of two-dimensional transition metal dichalcogenides," *Nat. Nanotechnol.* **7**, 699–712 (2012).
- ²⁹F. H. L. Koppens, T. Mueller, P. Avouris, A. C. Ferrari, M. S. Vitiello, and M. Polini, "Photodetectors based on graphene, other two-dimensional materials and hybrid systems," *Nat. Nanotechnol.* **9**, 780–793 (2014).
- ³⁰X. Zhu and D. R. Reichman, "2D materials," *J. Chem. Phys.* **154**, 040401 (2021).
- ³¹H. Duan, C. Wang, G. Li, H. Tan, W. Hu, L. Cai, W. Liu, N. Li, Q. Ji, Y. Wang, Y. Lu, W. Yan, F. Hu, W. Zhang, Z. Sun, Z. Qi, L. Song, and S. Wei, "Single-atom-layer catalysis in a MoS₂ monolayer activated by long-range ferromagnetism for the hydrogen evolution reaction: Beyond single-atom catalysis," *Angew. Chem., Int. Ed.* **60**, 7251–7258 (2021).
- ³²R. J. Yang, Y. Y. Fan, Y. F. Zhang, L. Mei, R. S. Zhu, J. Q. Qin, J. G. Hu, Z. X. Chen, Y. Hau Ng, D. Voiry, S. Li, Q. Y. Lu, Q. Wang, J. C. Yu, and Z. Y. Zeng, "2D transition metal dichalcogenides for photocatalysis," *Angew. Chem., Int. Ed.* **62**, e202218318 (2023).
- ³³A. Castellanos-Gomez, M. Buscema, R. Molenaar, V. Singh, L. Janssen, H. S. J. van der Zant, and G. A. Steele, "Deterministic transfer of two-dimensional materials by all-dry viscoelastic stamping," *2D Mater.* **1**, 011002 (2014).
- ³⁴M. Van Der Donck and F. M. Peeters, "Interlayer excitons in transition metal dichalcogenide heterostructures," *Phys. Rev. B* **98**, 115104 (2018).
- ³⁵E. Shafran, B. D. Mangum, and J. M. Gerton, "Using the near-field coupling of a sharp tip to tune fluorescence-emission fluctuations during quantum-dot blinking," *Phys. Rev. Lett.* **107**, 037403 (2011).
- ³⁶Z. He, Z. H. Han, J. T. Yuan, A. M. Sinyukov, H. Eleuch, C. Niu, Z. R. Zhang, J. Lou, J. Hu, D. V. Voronine, and M. O. Scully, "Quantum plasmonic control of trions in a picocavity with monolayer WS₂," *Sci. Adv.* **5**, eaau8763 (2019).
- ³⁷S. J. Haigh, A. Gholinia, R. Jalil, S. Romani, L. Britnell, D. C. Elias, K. S. Novoselov, L. A. Ponomarenko, A. K. Geim, and R. Gorbachev, "Cross-sectional imaging of individual layers and buried interfaces of graphene-based heterostructures and superlattices," *Nat. Mater.* **11**, 764–767 (2012).
- ³⁸L. Amirav and M. Wächtler, "Nano Schottky?," *Nano Lett.* **22**, 9783–9785 (2022).
- ³⁹G. Giovannetti, P. A. Khomyakov, G. Brocks, V. M. Karpan, J. van den Brink, and P. J. Kelly, "Doping graphene with metal contacts," *Phys. Rev. Lett.* **101**, 026803 (2008).
- ⁴⁰J. Sławińska, P. Dabrowski, and I. Zasada, "Doping of graphene by a Au(111) substrate: Calculation strategy within the local density approximation and a semiempirical van der Waals approach," *Phys. Rev. B* **83**, 245429 (2011).
- ⁴¹A. C. Aragonès, N. L. Haworth, N. Darwish, S. Ciampi, N. J. Bloomfield, G. G. Wallace, I. Diez-Perez, and M. L. Coote, "Electrostatic catalysis of a Diels–Alder reaction," *Nature* **531**, 88–91 (2016).
- ⁴²D. M. Zhang, X. Yuan, C. Gong, and X. X. Zhang, "High electric field on water microdroplets catalyzes spontaneous and ultrafast oxidative C-H/N-H cross-coupling," *J. Am. Chem. Soc.* **144**, 16184–16190 (2022).
- ⁴³S. Shaik, R. Ramanan, D. Danovich, and D. Mandal, "Structure and reactivity/selectivity control by oriented-external electric fields," *Chem. Soc. Rev.* **47**, 5125–5145 (2018).
- ⁴⁴S. Shaik, D. Danovich, J. Joy, Z. F. Wang, and T. Stuyver, "Electric-field mediated chemistry: Uncovering and exploiting the potential of (oriented) electric fields to exert chemical catalysis and reaction control," *J. Am. Chem. Soc.* **142**, 12551–12562 (2020).
- ⁴⁵M. Chubarov, T. H. Choudhury, D. R. Hickey, S. Bachu, T. Zhang, A. Sebastian, A. Bansal, H. Zhu, N. Trainor, S. Das, M. Terrones, N. Alem, and J. M. Redwing, "Wafer-scale epitaxial growth of unidirectional WS₂ monolayers on sapphire," *ACS Nano* **15**, 2532–2541 (2021).
- ⁴⁶T. T. Li, W. Guo, L. Ma, W. S. Li, Z. H. Yu, Z. Han, S. Gao, L. Liu, D. X. Fan, Z. X. Wang, Y. Yang, W. Y. Lin, Z. Z. Luo, X. Q. Chen, N. X. Dai, X. C. Tu, D. F. Pan, Y. G. Yao, P. Wang, Y. F. Nie, J. L. Wang, Y. Shi, and X. R. Wang, "Epitaxial growth of wafer-scale Molybdenum Disulfide semiconductor single crystals on sapphire," *Nat. Nanotechnol.* **16**, 1201–1207 (2021).
- ⁴⁷J. Wang, X. Xu, T. Cheng, L. Gu, R. Qiao, Z. Liang, D. Ding, H. Hong, P. Zheng, Z. Zhang, Z. Zhang, S. Zhang, G. Cui, C. Chang, C. Huang, J. Qi, J. Liang, C. Liu, Y. Zuo, G. Xue, X. Fang, J. Tian, M. Wu, Y. Guo, Z. Yao, Q. Jiao, L. Liu, P. Gao, Q. Li, R. Yang, G. Zhang, Z. Tang, D. Yu, E. Wang, J. Lu, Y. Zhao, S. Wu, F. Ding, and K. Liu, "Dual-coupling-guided epitaxial growth of wafer-scale single-crystal WS₂ monolayer on vicinal a-plane sapphire," *Nat. Nanotechnol.* **17**, 33–38 (2021).
- ⁴⁸H. Yu, M. Liao, W. Zhao, G. Liu, X. J. Zhou, Z. Wei, X. Xu, K. Liu, Z. Hu, K. Deng, S. Zhou, J.-A. Shi, L. Gu, C. Shen, T. Zhang, L. Du, L. Xie, J. Zhu, W. Chen, R. Yang, D. Shi, and G. Zhang, "Wafer-scale growth and transfer of highly-oriented monolayer MoS₂ continuous films," *ACS Nano* **11**, 12001–12007 (2017).